Available online at www.sciencedirect.com

SciVerse ScienceDirect

Ceramics International 39 (2013) 2869–2875

CERAMICS INTERNATIONAL

www.elsevier.com/locate/ceramint

An elevated temperature infrared emissivity ceramic coating formed on 2024 aluminium alloy by microarc oxidation

Y.M. Wang[a,*], H. Tian[a], X.E. Shen[b], L. Wen[a], J.H. Ouyang[a], Y. Zhou[a], D.C. Jia[a], L.X. Guo[a]

[a]*Institute for Advanced Ceramics, Harbin Institute of Technology, Harbin 150001, China*
[b]*Beijing Electro-mechanical Engineering Institute, Beijing 100074, China*

Received 25 August 2012; received in revised form 26 August 2012; accepted 17 September 2012
Available online 23 September 2012

Abstract

An infrared emissivity coating material containing γ-Al_2O_3 was prepared on 2024 aluminium alloy surface by the microarc oxidation (MAO) method. The microstructure of the coatings was analysed by SEM, XRD and EDS techniques. The infrared emissivity properties tested at 500 °C were investigated by an infrared radiometer based on a Fourier transform infrared spectrometer. The results show that the infrared emissivity values of coated Al samples depend on the phase composition and surface roughness of the coatings. Corresponding to increasing coatings thickness, the gradually increasing γ-Al_2O_3 content and some oxide compounds containing Si and P contribute to the higher infrared emissivity value (about 0.85) in the wavelength range of 8–20 μm. The increasing surface roughness leads to an obvious increase in emissivity from 0.2 to 0.4 at wavelength 3–5 μm.

Keywords: Aluminium alloy; Ceramic coating; Microstructure; Infrared emissivity

1. Introduction

Microarc oxidation (MAO) has been extensively investigated to fabricate a wide variety of ceramic coatings with designable chemical compositions on aluminium alloys for corrosion and wear resistance applications [1–11] depending on the inherent process characteristics. Most recently, it has produced potentially great microarc oxidation coatings used in elevated temperature application circumstances due to their excellent high temperature stability [12–15]. These potential application fields include aerocrafts, internal combustion engines, and heat exchangers, as well as metal/oxide layers for catalysis and the heat dissipation surface of electronic devices carrying backplanes in electronic industries (3C products). When serving in the elevated temperatures application circumstance, the heat transfer occurring on the aluminium alloy components includes conduction, convection and radiation. Conduction takes place in the metal bulk material while convection and radiation take place at the exterior surfaces. Heat transfer characteristic by infrared thermal radiation of aluminium alloy or their coatings plays a crucial role in the simulation calculation and design of radiation parameters for the purpose of thermal management.

Radiation heat transfer depends on the emissivity and its distribution in broad spectral wavelength range of exposed metal devices surface. Aluminium and its alloys have a low emissivity [16] over the whole spectrum and thus cannot dissipate heat by radiating in the thermal infrared region. It is well known that most polar bonding oxides show strong efficiency of photon emission thus exhibiting a high emissivity value. Microarc oxidation enables transformation of the surface of aluminium alloy into Al_2O_3 dominated oxides ceramic by spark discharging events, which has the potential to promote the emissivity value, thus enhancing the dissipation of heat by radiations. Unfortunately, the work concerning the research on infrared radiating properties of microarc oxidation coatings formed on alunimium alloys is scarse.

In this work, the ceramic coatings containing Al_2O_3 were fabricated on 2024 aluminium alloy surface by the microarc oxidation (MAO) method in an alkaline silicate solution. How the modified coating structure affects the infrared emissivity

*Corresponding author. Tel.: +86 451 86402040x8403; fax: +86 451 86412491.
E-mail address: wangyaming@hit.edu.cn (Y.M. Wang).

0272-8842/$ - see front matter © 2012 Elsevier Ltd and Techna Group S.r.l. All rights reserved.
http://dx.doi.org/10.1016/j.ceramint.2012.09.060

property is not clear. Thus, this work focuses on the relationships between the specially modified layers microstructure and the infrared emissivity of MAO coated aluminium alloy. Additionally, the oxidation effect of uncoated aluminium sample surface has also been taken into consideration, so the changes of infrared emissivity properties with increasing exposure time of the uncoated aluminium alloy were also presented.

2. Experimental

2.1. Coating preparation

The material used in the experiment is 2024 Al alloy with nominal composition 4.36% Cu, 1.49% Mg, 0.46% Mn, 0.25% Fe, 0.14% Si, 0.07% Zn, 0.01% Ti and rest Al. Samples for infrared emissivity testing cut into a disc (30 mm diameter and 1 mm thick) were used as the substrate. The surface of the samples was polished with 400#, 800# and 1200# abrasive papers to a roughness of $R_a \approx 0.2$ μm, and ultrasonically cleaned in distilled water followed by ethanol and dried. The samples were used as anodes, while stainless steel plates were used as cathodes in the electrolytic bath.

The pretreated samples were subjected to microarc oxidation treatment according to the following conditions. The based electrolyte of alkaline silicate was prepared from the solution of Na_2SiO_3 (6.0 g/L), NaOH (1.2 g/L), $(NaPO_3)_6$ (35.0 g/L) and other additives in distilled water. A 65 kW microarc oxidation device provides the voltage waveform. The electrical parameters were fixed as follows: voltage 600 V, frequency 600 Hz, and duty cycle 10.0%. In the experiments, the test samples with three values of coating thickness (5, 10 and 15 μm) were fabricated using different oxidation time periods by MAO treatment.

2.2. Coating characterisation

The coating thickness was measured with a coating thickness gauge (Minitest 600B, Germany EPK). The surface roughness of the coatings was determined by a profile and roughness tester (JB-4C, Shanghai Optical Instrument Co.) The surface and cross section morphologies of coatings were observed using scanning electron microscopy (SEM, S4800, Hitachi Co.). The phase composition of the coatings was analysed by X-ray diffraction (XRD, Philips X'Pert) using CuK_α radiation at a grazing angle of 3°.

2.3. Emissivity measurements

Infrared emissivity values of the samples were carried out on a self-made infrared radiometer based on a Fourier transform infrared spectrometer. The radiation emitted by the sample front surface is detected by a Fourier transform infrared (FT-IR) spectrometer (JASCO FT/IR-6100), and its radiance is compared with the radiance of a reference blackbody radiator. In this way the infrared emissivity value of sample is obtained based on the principle of radiation comparison with sample radiance to blackbody radiance. The spectral emissivity was determined by comparing the radiative fluxes of a sample and a blackbody radiation under the same conditions. The FTIR spectrometer used in this experiment can rapidly scan spectra at a high spectral resolution and broad wavelength range of 3–20 μm. Detailed test method can be found in our previous publication [17].

Once the coated aluminium sample temperature is stable at 500 °C, the sample spectrum is acquired, next, the reference blackbody signal is measured, and thus the emissivity is obtained. To investigate the effect of surface oxidation on the metal aluminium on the infrared emissivity, the uncoated aluminium sample is mounted with exposure to the tested temperature and the sample spectrum is instantly acquired. Subsequently, a series of sample spectra are acquired at 30 s interval with increasing exposure time till the sample spectrum does not change any more. The estimated uncertainty for the emissivity measurement is less than 5%.

3. Results and discussion

3.1. Microstructure of coating

The XRD patterns of MAO coatings with different thicknesses formed on 2024 Al alloy are shown in Fig. 1. It can be found that γ-Al_2O_3 phase is the main composition for the different coatings, and the intensity of γ-Al_2O_3 peak increases obviously with the thickening of the coating from 5 μm through 10 μm to 15 μm. However, depending on the relatively small thickness of the coatings, X-rays can penetrate through the coating which leads to the diffraction peaks of Al alloy substrate to be reflected in the XRD patterns.

The surface morphologies of MAO coatings with different thicknesses formed on 2024 Al alloy are illustrated in Fig. 2. MAO coating is characterised by a typical surface

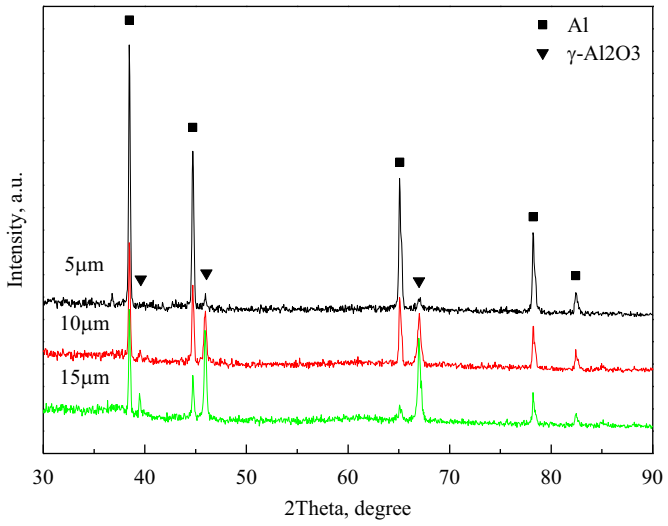

Fig. 1. XRD patterns of MAO coatings with different thicknesses formed on 2024 Al alloy.

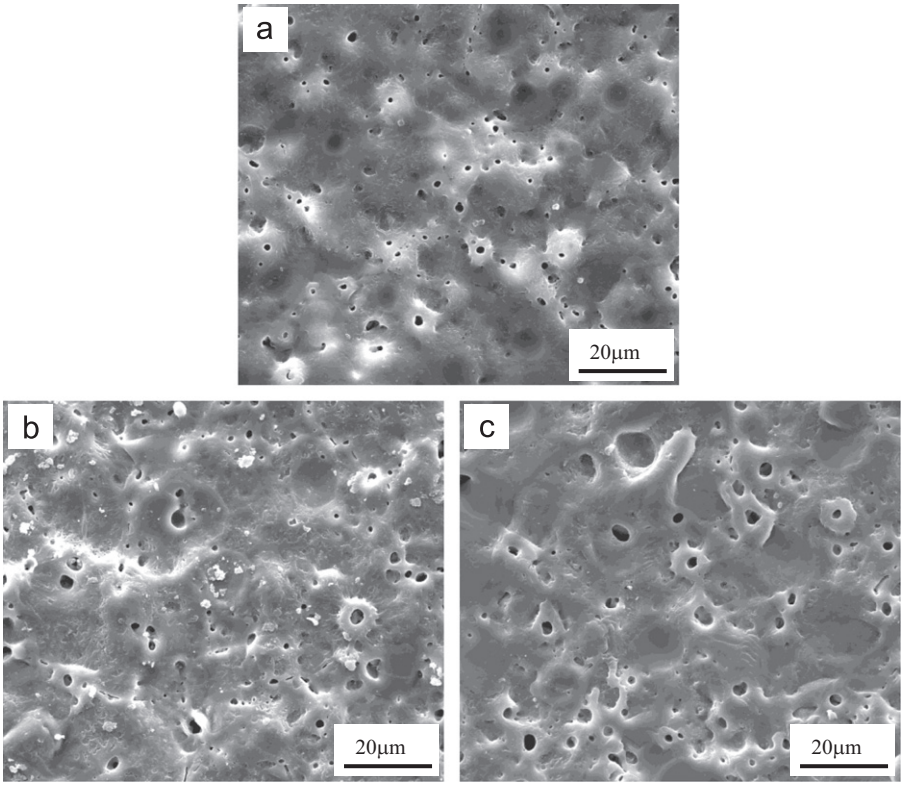

Fig. 2. Surface morphologies of MAO coating with different thicknesses formed on 2024 Al alloy: (a) 5 μm, (b) 10 μm, and (c) 15 μm.

scattered with many micropores, which are the high-voltage spark discharge tunnels formed by the rapid cooling of the coating in the electrolyte, as shown in Fig. 2 a–c. And the size of pores remaining after sparks decayed slightly increases with the thickening of the coating from 5 μm through 10 μm to 15 μm. Therefore, the increasing pore size inevitably leads to increasing rough surface morphology, and the corresponding average roughness registers as R_a 1.02 μm, R_a 1.20 μm and R_a 1.35 μm for 5, 10 and 15 μm thick coatings, respectively, as shown in Fig. 3. In comparison, the surface roughness of the uncoated substrate after grinding by SiC sand paper is as low as R_a 0.22 μm.

Fig. 4 illustrates the cross-section morphologies and elements distribution of MAO coated 2024 Al alloy. It can be found that the coatings are compact and bond well with the substrate. With the increase of coating thickness from 10 to 15 μm, the coating/substrate interfaces become slightly uneven. The phenomenon can be attributed to the excessive growth of the coating in the local ever discharging region. Analysis of elements distribution along the cross-section showed that the oxygen content of the coating significantly increased, indicating that the MAO coating contains a lot of aluminium oxide, corresponding to the results of XRD. Meanwhile, the MAO coating also consists of Si and P elements, which are the components from the electrolyte. It should be noticed that Si element is evenly distributed along the coating thickness, while the P element is mainly distributed near the interface. However, the coating compounds containing Si and P have not been

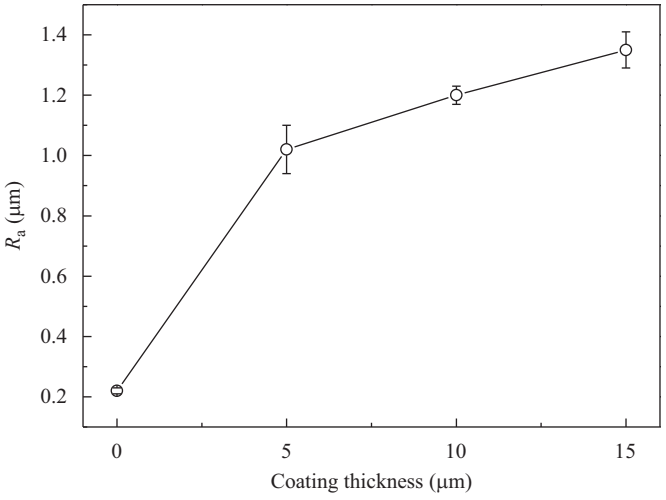

Fig. 3. Surface roughness of MAO coating with different thicknesses formed on 2024 Al alloy.

detected in the XRD pattern, which is possibly attributed to their low content.

3.2. Infrared emissivity properties

It has been proved that electron–phonon aharmonicities may play a role in the observed dependence [18], and each oxide has a specific emissivity distribution in the range of infrared spectrum. Fig. 5 shows the spectral emissivity

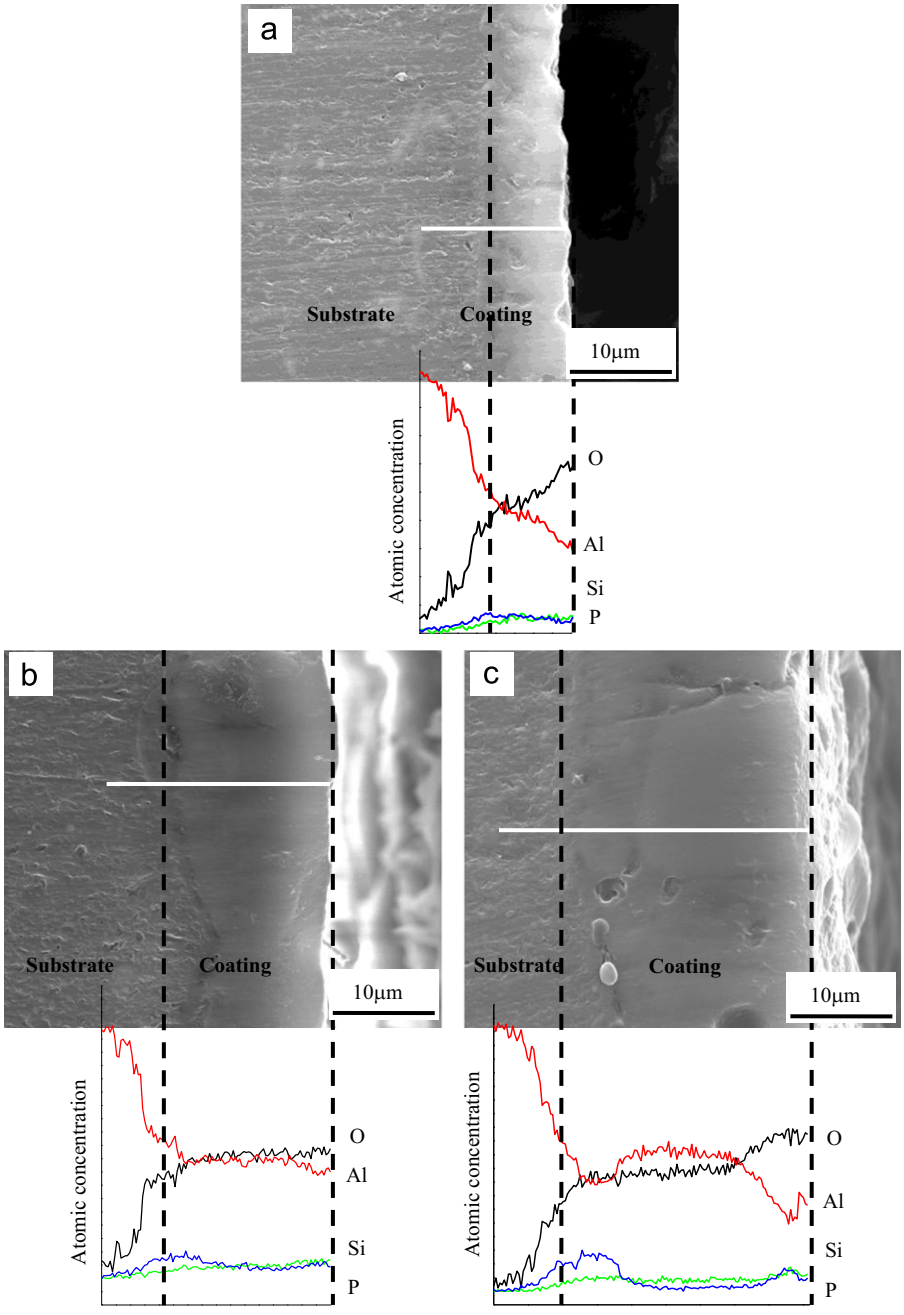

Fig. 4. Cross-section morphologies and elements distribution of microarc oxidation coatings with different thicknesses formed on 2024 Al alloy: 5 μm, (b) 10 μm, and (c) 15 μm.

distribution of sintered Al_2O_3 ceramic [19] and Al_2O_3 dominated microarc oxidation coatings. It is rather obvious that the pure Al_2O_3 ceramic has a unique emissivity distribution with a gradual increase from 0.2 to 0.85 at wavelength 3–8 μm, almost maintaining a high constant of 0.88 at wavelength 8–12 μm, and then gradually decreasing to 0.6 at wavelength 12–15 μm. In comparison, the Al_2O_3 dominated microarc oxidation coatings indicated a different changing evolution of emissivity. At wavelength 3–12 μm, the emissivity for microarc oxidation coating shows a similar change as that of the the sintered Al_2O_3 ceramic, except for the increased values in wavelength 3–6 μm. The increased emissivity is attributed to the increasing surface roughness for the microarc oxidation coating. And it is worth noting that at wavelength 12–20 μm, the emissivity has a significant increase for the microarc oxidation coating when compared with the sintered Al_2O_3 ceramic, which is possibly caused by the incorporated compounds containing Si and P.

Emissivity is a property which reveals how much radiation a given body emits as compared to a blackbody. When tested in atmosphere, the H_2O (room humidity) and CO_2 existing in atmosphere affect the spectral emissivity. It can be seen from Fig. 6 that the two shaded regions in each plot correspond to bands of appreciable atmospheric absorption

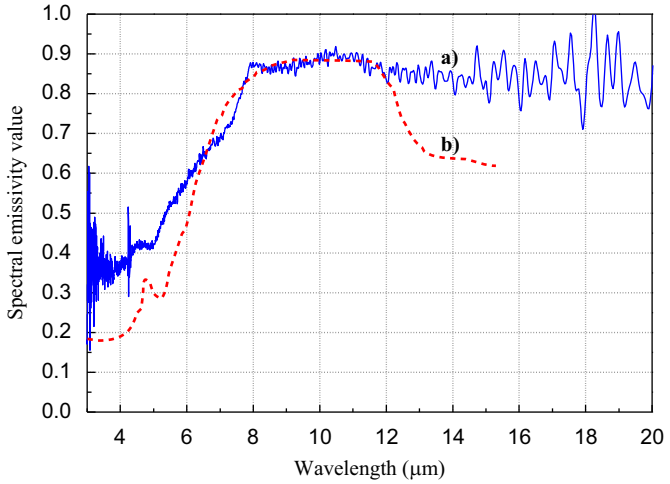

Fig. 5. Spectral emissivity comparison of Al_2O_3 dominated microarc oxidation coatings and sintered Al_2O_3 ceramic plate from Ref. [19].

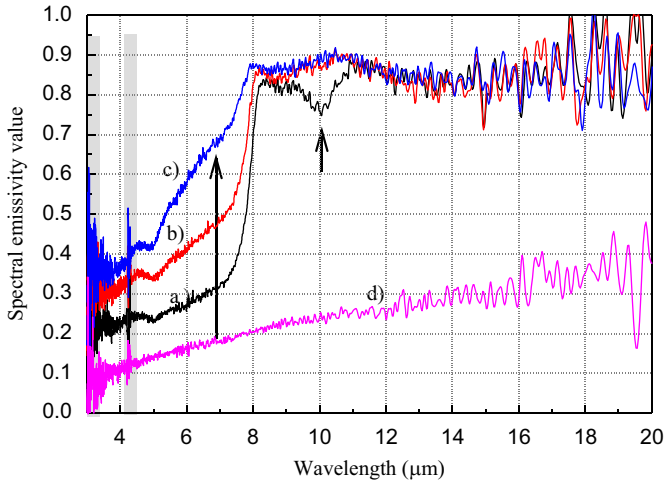

Fig. 6. Spectral emissivity values measured at wavelength 3–20 μm and 500 °C for microarc oxidation coatings with different thicknesses formed on aluminium alloy samples: (a) 5 μm; (b) 10 μm; (c) 15 μm; and (d) Al substrate.

and scattering. The first band (centred at 2.7 μm) is influenced by H_2O (room humidity) and CO_2 molecules, and the other (centred at 4.3 μm) by CO_2 molecules alone.

The emissivity value is highly influenced by the surface state, including inorganic components and surface roughness. It has been demonstrated in Section 3.1 that the microarc oxidation coatings with increasing thickness have gradually increasing γ-Al_2O_3 content and slightly increasing surface roughness. Therefore it is rather necessary to indicate the effects of phase composition and surface roughness on emissivity.

Fig. 6 shows the spectral emissivity values measured at wavelength 3–20 μm and 500 °C for microarc oxidation coatings with different thicknesses formed on aluminium alloy. It was found from Fig. 6 that the coating exhibits a higher infrared emissivity value (about 0.85) in the wavelength range of 8–20 μm than at that the lower wavelength of 3–8μm. However, with increasing coating thickness from 5 to 15 μm, the significant promotion of emissivity value at wavelengths 5–8 μm and 9–11 μm (indicated by rising arrows in Fig. 6) is from the contribution of increasing γ-Al_2O_3 phase content.

The coating surface roughness is one factor that affects the surface infrared scattering, according to the general theory of scattering is that the rougher the surface, the stronger the backscattering [20,21]. With the surface roughness increasing from R_a 1.02 μm through R_a 1.20 μm to R_a 1.35 μm for 5, 10 and 15 μm thick coating, the spectral emissivity value exhibits an obvious increase from 0.2 to 0.4 at the wavelength of 3–5 μm.

In addition, it is found that once the coated aluminium sample temperature is stable at the desired temperature of 500 °C, onintentionally increasing the exposure holding time the acquired radiation spectrum of the coated sample remains unchanged, which implies that the coating has a high thermal stability. Comparatively, the uncoated aluminium alloy shows a much lower infrared emissivity value of about 0.1–0.3 at 3–20 μm (as shown in Fig. 7), when the uncoated aluminium sample is mounted exposed at the tested temperature and the sample spectrum instantly acquired. In this case, the infrared emissivity contribution basically derives from the aluminium substrate, having inherently low emissivity values owing to the poor efficiency of photon emission from their surfaces.

However, the metal titanium surface is highly reactive and easily oxidised to form a thin Al_2O_3 film at the high temperature; therefore, on increasing exposure time to 30 s interval at 500 °C, the Al_2O_3 film thickness increases gradually which also leads to increase in infrared emissivity gradually from 0.1 for 30 s to 0.2 for 90 s at the beginning

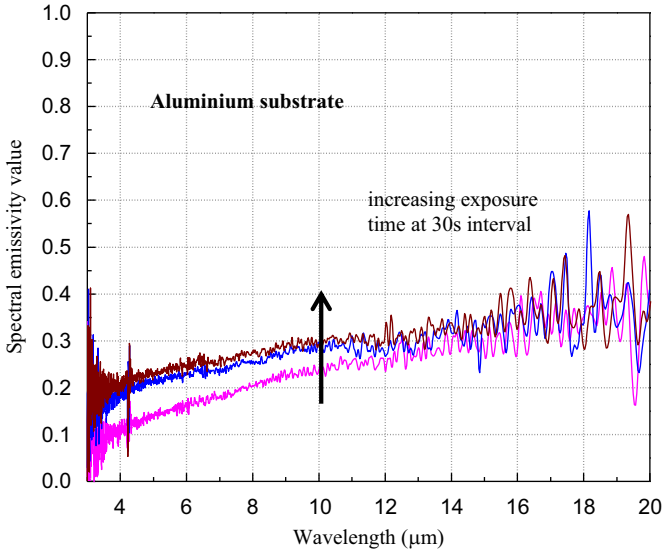

Fig. 7. Spectral emissivity value changes on increasing exposure time to 30 s interval at wavelength 3–20 μm and 500 °C for uncoated aluminium substrate sample.

wavelength, as shown in Fig. 7. The changing surface of Al_2O_3 film thickness accompanied by a visual change of surface colour from light metallic grey to black at 500 °C is believed to be the primary cause for the increased emissivity at this temperature. This discoloration is common to aluminium alloys which contain magnesium [22] such as the 2024 alloy.

It should be noted that the newly formed Al_2O_3 film is rather thin with several tens nm; thus the reflectance of aluminium metal substrate will also play the main contribution, which leads to the relatively low emissivity. Generally, the spectral emissivities of aluminium are found to increase with increasing wavelength and increase slightly with the increasing exposure time at high temperature. The gradually increasing γ-Al_2O_3 content and some oxide compounds containing Si and P contribute to the higher infrared emissivity value (about 0.85) in the wavelength range of 8–20 μm. MAO coated alunimium alloy can be used as infrared thermal radiation materials at elevated temperature. The obtained infrared thermal radiation characteristic of MAO coatings on aluminium alloy provides a powerful reference for the future simulation calculation and design of radiation parameters with the purpose of thermal management.

4. Conclusions

This study explored the effects of coating thickness, phase composition and surface roughness on spectral emissivity of microarc oxidised 2024 aluminium alloy. The key findings from the study are as follows:

(1) the gradually increasing γ-Al_2O_3 content and some oxide compounds containing Si and P contribute to the higher infrared emissivity value (about 0.85) in the wavelength range of 8–20 μm;
(2) the significant promotion of emissivity value at wavelengths 5–8 μm and 9–11 μm is from the contribution of the enhanced photon emission with increasing γ-Al_2O_3 phase content;
(3) the increasing surface roughness leads to an obvious increase of emissivity from 0.2 to 0.4 at the wavelength of 3–5 μm;
(4) the uncoated Al samples show lower emissivity value although exhibiting a slight increase from 0.1 to 0.3 with increasing exposure time at 500 °C.

Acknowledgements

The partial supports from the NSFC Grant nos. 51021002 and 50701014, the Programme for New Century Excellent Talents in University of China (NCET-08-0166) and the Fundamental Research Funds for the Central Universities (HIT. BRETIII.201202) are gratefully acknowledged.

References

[1] A.L. Yerokhin, X. Nie, A. Leyland, A. Matthews, S.J. Dowey, Review: Plasma electrolysis for surface engineering, Surface and Coatings Technology 122 (1999) 73–93.
[2] W.B. Xue, X.L. Shi, M. Hua, Y.L. Li, Preparation of anti-corrosion films by microarc oxidation on an Al–Si alloy, Applied Surface Science 253 (2007) 6118–6124.
[3] L. Wen, Y.M. Wang, Y. Zhou, J.H. Ouyang, L.X. Guo., D.C. Jia, Corrosion evaluation of microarc oxidation coatings formed on 2024 aluminium alloy, Corrosion Science 52 (2010) 2687–2696.
[4] S. Stojadinovic, R. Vasilic, I. Belca, M. Petkovic, B. Kasalica, Z. Nedic, Lj. Zekovic, Characterisation of the plasma electrolytic oxidation of aluminium in sodium tungstate, Corrosion Science 52 (2010) 3258–3265.
[5] H.H. Wu, J.B. Wang, B.Y. Long, B.H. Long, Z.S. Jin, N.D. Wang, F.R. Yu, D.M. Bi, Ultra-hard ceramic coatings fabricated through microarc oxidation on aluminium alloy, Applied Surface Science 252 (2005) 1545–1552.
[6] V. Raj, M. Mubarak Ali, Formation of ceramic alumina nanocomposite coatings on aluminium for enhanced corrosion resistance, Journal of Materials Processing Technology 209 (2009) 5341–5352.
[7] C.C. Tseng, J.L. Lee, T.H. Kuo, S.N. Kuo, K.H. Tseng, The influence of sodium tungstate concentration and anodizing conditions on microarc oxidation (MAO) coatings for aluminium alloy, Surface and Coatings Technology 206 (2012) 3437–3443.
[8] M.H. Zhu, Z.B. Cai, X.Z. Lin, P.D. Ren, J. Tan, Z.R. Zhou, Fretting wear behaviour of ceramic coating prepared by micro-arc oxidation on Al–Si alloy, Wear 263 (2007) 472–480.
[9] T.B. Wei, F.Y. Yan, J. Tian, Characterisation and wear- and corrosion-resistance of microarcoxidation ceramic coatings on aluminium alloy, Journal of Alloys and Compounds 389 (2005) 169–176.
[10] A. Polat, M. Makaraci, M. Usta, Influence of sodium silicate concentration on structural and tribological properties of microarc oxidation coatings on 2017A aluminium alloy substrate, Journal of Alloys and Compounds 504 (2010) 519–526.
[11] L.R. Krishna, K.R.C. Somaraju, G. Sundararajan, The tribological performance of ultra-hard ceramic composite coatings obtained through microarc oxidation, Surface and Coatings Technology 163-164 (2003) 484–490.
[12] S.V. Gnedenkov, O.A. Khrisanfova, A.G. Zavidnaya, S.L. Sinebrukhov, P.S. Gordienko, S. Iwatsubo, A. Matsui, Composition and adhesion of protective coatings on aluminium, Surface and Coatings Technology 145 (2001) 146–151.
[13] P.I. Butyagin, Y.V. Khokhryakov, A.I. Mamaev, Microplasma systems for creating coatings on aluminium alloys, Materials Letters 57 (2003) 1748–1751.
[14] S.V. Gnedenkov, O.A. Khrisanfova, A.G. Zavidnaya, S.L. Sinebrukhov, A.N. Kovryanov, T.M. Scorobogatova, P.S. Gordienko, Production of hard and heat-resistant coatings on aluminium using a plasma microdischarge, Surface and Coatings Technology 123 (2000) 24–28.
[15] J.A. Curran, T.W. Clyne, The thermal conductivity of plasma electrolytic oxide coatings on aluminium and magnesium, Surface and Coatings Technology 199 (2005) 177–183.
[16] C.D. Wen, I. Mudawar, Emissivity characteristics of roughened aluminium alloy surfaces and assessment of multispectral radiation thermometry (MRT) emissivity models, **International Journal of Heat** and **Mass Transfer** 47 (2004) 3591–3605.
[17] Z.W. Wang, Y.M. Wang, Y. Liu, J.L. Xu, L.X. Guo, Y. Zhou, J.H. Ouyang, J.M. Dai, Microstructure and infrared emissivity property of coating containing TiO_2 formed on titanium alloy by microarc oxidation, Current Applied Physics 11 (2011) 1405–1409.
[18] K. Nouneh, I.V. Kityk, R. Viennois, S. Benet, S. Charar, S. Paschen, K. Ozga, Influence of an electron–phonon subsystem on specific heat and two-photon absorption of the semimagnetic semiconductors $Pb_{1-x}Yb_xX$ (X=S, Se,Te) near the semiconductor–isolator phase transformation, Physical Review B 73 (2006) 035329.

[19] J.C. Richmond, C.R. Counts, Emittance of Sintered Oxides, AIAA Paper, no. 67-301, 1965.
[20] J.Y. Liu, C.F. Huang, P.C. Hsueh, Acoustic plane-wave scattering from a rough surface over a random fluid medium, Ocean Engineering 29 (2002) 915–930.
[21] I. Simonsen, A.A. Maradudin, Numerical simulation of electromagnetic wave scattering from planar dielectric films deposited on rough perfectly conducting substrates, Optics Communications 162 (1999) 99–111.
[22] M.J. Haugh, Radiation thermometry in the aluminium industry, in: D.P. DeWitt, G.D. Nutter (Eds.), Theory and Practice of Radiation Thermometry, John Wiley and Sons, NewYork, 1988.